CHEMISTRY
A EUROPEAN JOURNAL

DOI: 10.1002/chem.200801549

Phosphorus-Based Heteropentacenes: Efficiently Tunable Materials for Organic n-Type Semiconductors

Yvonne Dienes,[a] Matthias Eggenstein,[a] Tamás Kárpáti,[b] Todd C. Sutherland,[c] László Nyulászi,*[b] and Thomas Baumgartner*[a, c]

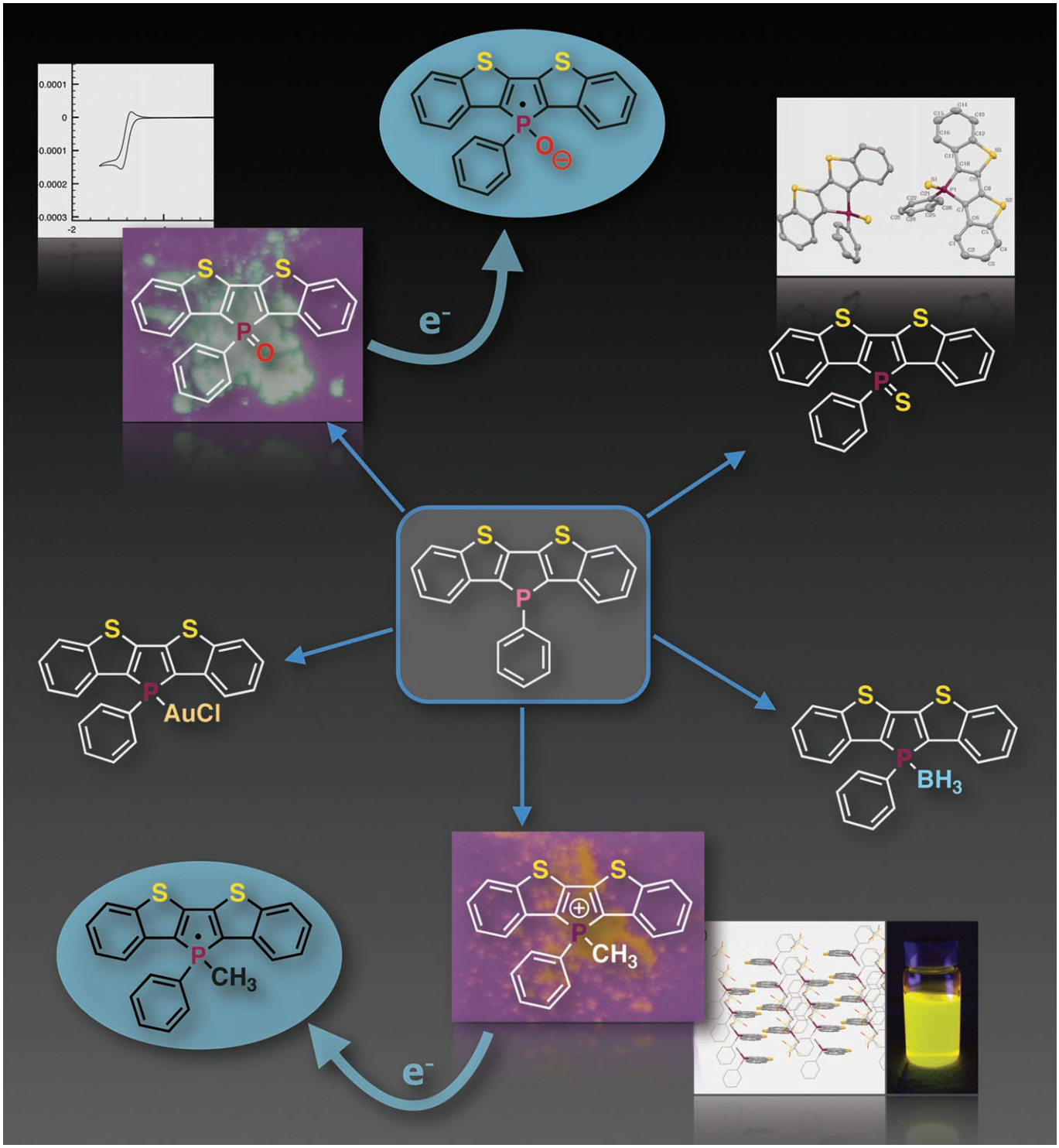

Abstract: Benzo-condensed dithieno[3,2-*b*:2′,3′-*d*]phospholes have been synthesized that allow convenient tuning of properties that are essential for application as semiconductor materials in organic field-effect transistor (OFET) devices. The versatile reactivity of the trivalent phosphorus atom in these heteropentacenes provides access to a series of materials that show different photophysical properties, significantly different organization in the solid state, and distinctly different electrochemical properties that can be achieved by simple chemical modifications. The materials show strong photoluminescence in solution and in the solid state that depends on the electronic nature of the phosphorus center. Electrochemical studies revealed that the phosphorus atom intrinsically furnishes materials with n-channel or ambipolar behavior, also depending on its electronic nature. The experimental data were verified by DFT quantum chemical calculations and suggest that the phosphorus-based heteropentacenes could be excellent candidates for n-channel OFET semiconductor materials.

Keywords: density functional calculations · luminescence · phosphorus heterocycles · semiconductors · sulfur heterocycles

Introduction

Organic π-conjugated oligomers and polymers exhibit semiconducting properties and hence are used increasingly as active materials in organic field-effect/thin-film transistors (OFET/OTFTs),[1,2] organic light-emitting diodes (OLEDs),[2–4] photovoltaic cells,[5] and sensor materials.[6] The organic nature of these materials, when suitably modified, allows for low-cost deposition processes such as printing, stamping, spin coating, and evaporation, and expensive lithographic or vacuum-deposition steps are not required.[7] Low-temperature solution processing, in particular, expands the repertoire of tolerant substrates and allows fabrication of flexible, lightweight, and inexpensive devices.[3,6a] A great deal of attention has been focused on modification of the electronic nature of the materials to obtain properties suitable for the desired function (high charge-carrier mobility, electroluminescence, etc.). The band gap of organic materials and the degree of π-conjugation can generally be adjusted by chemical transformations to tailor the optoelectronic properties of these materials; these modifications can also significantly influence their organization in the solid state.[2,8] The solid-state morphology of conjugated materials, in particular, plays an important role in the performance characteristics of electronic devices.[2,6a,9] Both exciton migration and carrier mobility strongly depend on the solid-state packing of the conjugated system. Greater intermolecular overlap leads to increased bandwidth, which is directly related to carrier mobility.[10] Pentacene was one of the first organic materials successfully employed in OTFTs and shows high field effect mobility and properties comparable to those of classical transistors that rely on amorphous silicon as active material.[2] However, due the low solubility and poor stability of pentacene towards oxidation, investigations focusing on improved materials that circumvent these problems have been performed.[1,2] Heteropentacenes containing annelated thiophene moieties such as pentathienoacenes (PTA),[11] tetraceno[2,3-*b*]thiophene (TCT),[12] and anthradithiophene (ADT)[13], for example, were found to exhibit higher stability than the parent pentacene and also exhibit good FET performance. However, most of these materials require tedious syntheses and purification processes. Recently, dibenzo[*d*,*d*′]thieno[3,2-*b*;4,5-*b*′]dithiophene (DBTDT) was investigated as a new material for organic electronics and showed not only promising semiconducting properties, but also high thermal and photostability, as well as easy accessibility.[14]

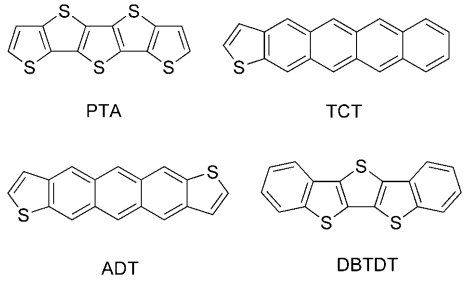

In the context of organic electronics, incorporation of phosphorus centers into oligomeric or macromolecular materials has also recently drawn significant attention.[15] Phosphole-containing materials are of particular interest. In contrast to planar pyrroles, due to the pyramidal environment of the tricoordinate phosphorus center, efficient orbital interaction of the phosphorus lone pair with the conju-

[a] Dr. Y. Dienes, M. Eggenstein, Prof. Dr. T. Baumgartner
Institute of Inorganic Chemistry, RWTH-Aachen University
Landoltweg 1, 52074 Aachen (Germany)
E-mail: thomas.baumgartner@ucalgary.ca

[b] Dr. T. Kárpáti, Prof. Dr. L. Nyulászi
Department of Inorganic and Analytical Chemistry
Budapest University of Technology and Economics
1521 Budapest Gellért tér 4 (Hungary)
Fax: (+36) 1463-3363
E-mail: nyulaszi@chem.bmu.hu

[c] Prof. Dr. T. C. Sutherland, Prof. Dr. T. Baumgartner
Department of Chemistry, University of Calgary
2500 University Drive NW, Calgary, AB T2N 1N4 (Canada)
Fax: (+1) 403-289-9488

Supporting information for this article is available on the WWW under http://dx.doi.org/10.1002/chem.200801549.

gated system is inhibited, and a low degree of lone-pair delocalization results (Figure 1).[16] In addition, the phosphole system exhibits a peculiar electronic structure resulting from

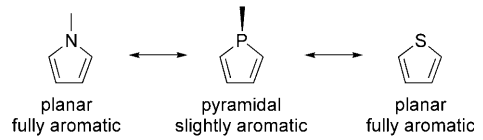

Figure 1. Pyrrole versus phosphole versus thiophene.

some interaction between the endocyclic π system of the butadiene moiety and the σ* orbital of the exocyclic P–C bond (σ–π hyperconjugation).[17] This interaction leads to a low-lying LUMO energy level that is particularly attractive for organic electronics with respect to n-channel (or n-type) semiconducting behavior. Furthermore, trivalent phosphorus species can react with oxidizing agents or Lewis acids, and they can also coordinate to transition metals.[18] This offers a variety of synthetically facile possibilities that can be used to efficiently modify the electronic properties of the product materials.[19] Réau and co-workers were among the first to incorporate the phosphole moiety into extended π-conjugated materials (**A**);[15,20] their systematic studies demonstrated the advantageous electronic features of the incorporated phosphorus centers in a series of phosphole-based OLED devices.[21]

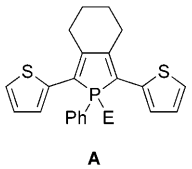

A

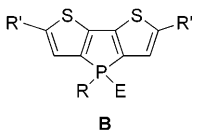

B

A few years ago, we introduced the dithieno[3,2-*b*:2′,3′-*d*]phosphole system **B** into the field of organic electronics.[22] This building block conjoins two thiophene subunits with a central phosphole moiety by annelation and allows selective tuning of the electronic properties of the materials by functionalization of the phosphorus atom.[19e] Fused bithiophene materials in general are promising candidates for application in organic electronics, as they provide a high degree of π conjugation due to their rigidified, planar structure, which intrinsically affords smaller HOMO–LUMO gaps.[8,23] Our extensive, systematic investigations to date have revealed that this is also true of the dithienophosphole system **B**, and we were able to confirm a doping function of the phosphorus center, rather than its being an integral part of the π-conjugated system.[19e,22] The materials obtained in our studies display highly advantageous, unprecedented photophysical properties with respect to emission wavelengths, intensity, and tunability. Parent dithienophospholes are very strong blue-light emitters with photoluminescence efficiencies of up to 90%. Notably, their photophysical properties can efficiently be tuned by simple modifications at either the phosphorus center (E = lone pair) by oxidation (E = O, S), complexation with main group centers (E = BH_3, CH_3^+) or transition metals (E = metal), or by variation of the substitution pattern (R′ on the thieno units or R on the central phosphorus atom).[19e,22,24]

We now report the synthesis and properties of heteropentacenes based on the dithieno[3,2-*b*:2′,3′-*d*]phosphole system with potential application in OFET/OTFT devices in mind. Expanding the π-conjugated framework over five rings, as opposed to the three rings of the parent dithienophosphole system, is expected to lead to improved intermolecular packing, better π overlap, and higher thermal stability, all of which are of central importance for the target application. Not only we will show that the central trivalent phosphorus atom plays an important part in tuning the electronic properties, but it also has a central role in the solid-state organization of the materials. Furthermore, interaction of the low-lying σ* P–C orbital with the low-lying unoccupied orbitals of the extended π* system is expected to facilitate n-channel conductivity in these compounds. The phosphorus center is thus a tool for efficiently and effectively tuning a range of materials properties, commonly not possible in this simplicity with genuine organic semiconductors.

Results and Discussion

Synthesis and photophysical properties: In a modified procedure reported by Dahlmann and Neidlein,[25] oxidative coupling of lithiated 2,3-dibromobenzo[*b*]thiophene (**1**) with copper(II) chloride in diethyl ether at −78 °C gave 3,3′-dibromo-2,2′-di(benzo[*b*]thiophene) (**2**). Benzannelated phosphole **3** was obtained in good yield by our general route to dithienophospholes[22,24] by using *n*BuLi in the presence of *N*,*N*,*N*,*N*-tetramethylethylenediamine to lithiate the 3,3′-positions, followed by treatment of the dilithio intermediate with phenyldichlorophosphane in diethyl ether at −78 °C (Scheme 1).

Compared to parent dithienophosphole **B** (R = Ph, R′ = H, E = lone pair),[22a] extension of the dithieno backbone does not have a great impact on the ^{31}P NMR shift of **3**, and a singlet at $\delta = -25.1$ ppm comparable to the signal for the parent compound ($\delta = -21.5$ ppm) is observed. This pentacene-analogous, rigid annelated ring system has a high

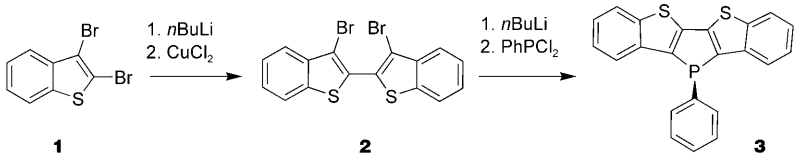

1 **2** **3**

Scheme 1. Synthesis of benzannelated phosphole **3**.

degree of π conjugation that is evident in bright blue fluorescence emission at $\lambda_{em}=440$ nm in solution. Compared with the parent dithienophosphole ($\lambda_{em}=415$ nm), the band gap of **3** is narrower, as expected;[22] its quantum yield is also reasonably high (63%). Remarkably, phosphole **3** shows extensive fluorescence, not only in solution but also in the solid state ($\lambda_{ex}=450$, $\lambda_{em}=512$ nm), for which a bright green emission can be observed that suggests some intermolecular interactions in the solid state (vide infra).

As mentioned in the introduction, the central phosphorus atom provides a means to efficiently manipulate the materials by simple chemical modifications that provide convenient access to a family of materials with significantly altered optoelectronic properties.[15,19e] Oxidation of the phosphorus center in **3** with hydrogen peroxide and sulfur gives **4** and **5**, respectively, as air-stable solids in nearly quantitative yields (Scheme 2). The phosphorus(V) ^{31}P NMR resonances show

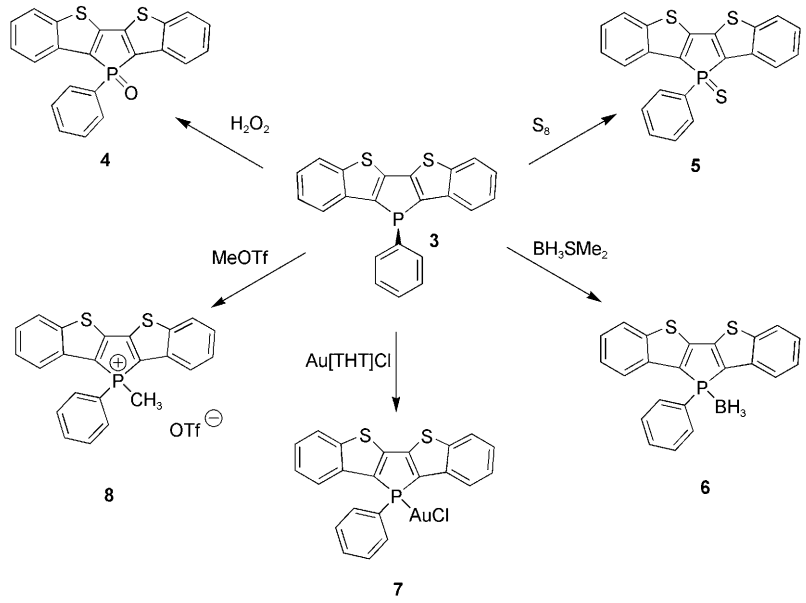

Scheme 2. Derivatization of benzannelated phosphole **3**.

the typical low-field shift (**4**: $\delta=16.6$ ppm; **5**: $\delta=23.1$ ppm) relative to the trivalent phosphole **3**.[19e,22,24] The optoelectronic properties of **4** and **5** are very similar, but in the solid state the relative intensity of **5** is significantly weaker, which is consistent with other related thio derivatives, due to the softness of sulfur (versus oxygen) quenching the luminescence.[22b] In solution, both compounds show excitation maxima at $\lambda_{ex}=424$ nm (**4**) and $\lambda_{ex}=435$ nm (**5**) and emission at $\lambda_{em}=483$ nm (**4**) and $\lambda_{em}=473$ nm (**5**) that are redshifted compared to trivalent phosphole **3**, as is commonly observed for dithienophospholes.[19e,22,24] This redshift is caused by the lowered LUMO level in the oxidized, pentavalent phosphorus form, as we showed in earlier studies on related dithienophospholes.[22b,24e]

Borane adduct **6** was formed by addition of BH_3 to phosphole **3**. The ^{31}P NMR resonance at $\delta=16.9$ ppm indicates that the electronic nature of the phosphorus atom is very similar to that of oxidized species **4** ($\delta(^{31}P)=16.6$ ppm). The excitation and emission maxima ($\lambda_{ex}=407$ nm, $\lambda_{em}=461$ nm) lie between those observed for phosphole **3** and oxidized species **4**, in accordance with the observations made for the parent dithienophospholes and their oxidized relatives (**B**: R=Ph, R′=H, SiR_3, E=O). The broad ^{11}B NMR signal at $\delta=-39.3$ ppm further indicates formation of **6**, by analogy with related boron dithienophosphole compounds ($\delta(^{11}B)=-40\pm1$ ppm).[22,24e]

Addition of [Au(tht)Cl] (tht=tetrahydrothiophene) to phosphole **3** in dichloromethane at room temperature gave gold complex **7** in 56% yield. Again, the low-field shift of the ^{31}P NMR resonance is in accordance with increased electron-acceptor character ($\delta=2.4$ ppm) and is comparable to the ^{31}P NMR resonances of related dithienophosphole gold complexes ($\delta=1.9$–6.5 ppm).[24b,e] The fluorescence spectrum for complex **7** also shows redshifted wavelengths of excitation and emission ($\lambda_{ex}=398$ nm, $\lambda_{em}=471$ nm). However, low-energy transitions that indicate aurophilic interactions[21] could not be observed in the fluorescence spectra of this compound. This observation is consistent with other dithienophosphole gold complexes reported by us earlier.[24d,e]

Methylation of the phosphorus center with methyl triflate generates air- and water-stable cationic phospholium compound **8**. Reaction of **3** with methyl iodide as methylating agent was significantly slower. The ^{31}P NMR spectrum of **8** shows a singlet at $\delta=13.2$ ppm that is significantly shifted from that of the starting material **3** ($\delta=-25.1$ ppm) and is characteristic for dithienophospholium compounds.[24d] Compound **8** exhibits yellow fluorescence in solution ($\lambda_{ex}=433$, $\lambda_{em}=520$ nm) with the largest redshift of this family of materials, due to the cationic nature of the phosphorus atom, which makes it an exceptionally strong acceptor center. The higher wavelength emission maximum of **8** with respect to dithienophospholium salt **B** (R=Ph, R′=H, E=Me^+),[24d] and derivative **A** (E=Me^+) investigated by Réau et al.[20c] indicates further lowering of the LUMO level in combination with an extensively delocalized π system in **8**.

All benzannelated compounds **3**–**8** show fluorescence in the solid state. The common quenching effect of neighboring molecules in the solid state is not observed.[26] This can be attributed to the bulky structure around the tetrahedral phosphorus center, which prevents extended π overlap of

neighboring molecules. The solid-state excitation and fluorescence emission of all compounds are further redshifted from solution (λ_{ex} = 436–506 nm, λ_{em} = 491–554 nm; for details, see Table 1), which is indicative of some intermolecular interactions, likely through π-stacking (vide infra). However, the solid-state fluorescence data do not show a similar trend to that in solution, in which shifts in the fluorescence data depend on the nature of the phosphorus center. Apparently, intermolecular interactions dominate the fluorescence properties in the solid state and surmount the impact of the phosphorus center on the photophysics of the materials. The experimental optoelectronic data of benzannelated derivatives **3**–**8** and the computed values are summarized in Table 1.

Table 1. Experimental and theoretical optical spectroscopic data for **3**–**8**.

	λ_{ex} [nm][a]	λ_{em} [nm][b]	φ_{PL} [%]	λ_{ex} [nm][e]	λ_{em} [nm][e]
3	385	440	63[c]	290, 420, *450*	512
calcd	315, 325, *375* (0.39[f])				
4	347, *424*	483	68[c]	419, *452*	509
calcd	321, 325, *407* (0.29[f])				
5	370, *435*	473	72[c]	456	498
calcd	324, 374, *422* (0.14[f])				
6	407	461	51[c]	421, *444*	491
7	338, *398*	471	63[c]	356, *436*	502
8	275, 362, *426*	520	31[d]	495	554
calcd	363, 365, *445* (0.20[f])				

[a] λ_{max} for excitation in CH_2Cl_2(π–π* HOMO–LUMO transition in italics). [b] λ_{max} for emission in CH_2Cl_2. [c] Fluorescence quantum yield relative to quinine sulfate (0.1 M H_2SO_4 solution), ±10%, excitation at 365 nm. [d] Fluorescence quantum yield, relative to rhodamine 101 (0.1 mM EtOH solution), ±10%, excitation at the excitation maximum (426 nm). [e] Excitation (π–π* HOMO–LUMO transition in italics) and emission in the solid state. Calculated values are vertical excitation energies at the TDDFT B3LYP/6-31G* level. [f] Intensity.

Solid-state structures: The solid-state morphology of conjugated materials plays an important role in the performance characteristics of electronic devices.[2,6a,9] If charge transport occurs by a hopping mechanism, then the hopping rate constant is also increased through a shorter distance and increased overlap of electron density between neighboring molecules.[27] Structural analysis of established OFET materials, such as pentacene and sexithiophene, show a herringbone motif in which the molecules are packed in an edge-to-face two-dimensional layer.[1,2,28] However, π–π overlap between adjacent molecules is minimized in this type of solid-state arrangement. Intermolecular interaction is increased by a face-to-face arrangement of the conjugated molecules. The presence of π stacking can be inferred from X-ray analysis; the typical interplanar distance for π stacking is 3.4–3.6 Å.[2,29] Most strategies to alter the features of pentacenes and their derivatives are based on changing the solid-state order from an edge-to-face (herringbone) arrangement to a face-to-face arrangement that allows π stacking.[2] Recent studies have explored the effect of solid-state order on the electronic properties of films and crystals.[9] As a result, new and improved pentacene-based materials have been developed for FETs[1,2] and LEDs.[30] Since packing properties and molecular interactions have a major impact on potential performance in OFET devices, the solid-state structures of heteropentacenes **4**, **5**, and **8** were investigated. These air- and moisture-stable materials are soluble in a variety of organic solvents, so solution processing for fabrication of OFET devices may be possible. Moreover, preliminary differential scanning calorimetry (DSC) studies on **4** and **5** showed significant thermal stability for both compounds, which decompose only at temperatures above 400 °C (**4**: 454 °C; **5**: 430 °C) and have a much lower melting/sublimation point (**4**: 252 °C; **5**: 232 °C), which potentially would also allow vapor-phase deposition onto OFET devices.

Single crystals of heteropentacene phosphole oxide **4** that were suitable for an X-ray diffraction study were obtained from a concentrated solution of **4** in acetone at room temperature. Compound **4** has a single molecule in the unit cell (Figure 2). All bond lengths and angles of **4** are comparable to those observed for previously reported dithienophosphole derivatives,[22,24] and the slight differences in bond-length alternation in **4** can be explained by further extension of the π-conjugated system over five ring subunits. Compound **4** shows intermolecular interactions between the oxygen and two sulfur atoms of neighboring molecules (Figure 2, bottom; 2.78 and 2.80 Å). This solid-state arrangement could prove useful for potential application in OFETs. As carrier transport in organic solids is governed by intermolecular overlap, it can also be enhanced by chalcogen–chalcogen contacts.[31] Likely as a result of these O···S interactions, the solid-state packing motif of **4** exhibits an edge-to-face herringbone-type arrangement of molecules (Figure 2, middle). In addition, the layers within the structure themselves show some π-stacking interactions in which two/three carbon atoms of the terminal benzene rings of adjacent molecules overlap (3.54 and 3.78 Å, see Supporting Information).

Heteropentacene phosphole sulfide **5**, crystallized from a concentrated solution of **5** in pentane at room temperature, has two independent molecules in the unit cell (Figure 3, top). Each has bond lengths and angles similar to those observed for **4**. Surprisingly, intermolecular chalcogen–chalcogen interactions are not observed in the solid-state arrangement. This may be because the sulfide sulfur atom is too large to fit between the two thiophene sulfur atoms of a neighboring molecule, unlike the oxygen atom in **4**. However, the coplanar arrangement of the dithienophosphole backbone in sulfur derivative **5** leads to π-stacking interactions in two dimensions (interplane distance 3.6 Å) between neighboring molecules of the same identity in the unit cell (Figure 3, bottom).

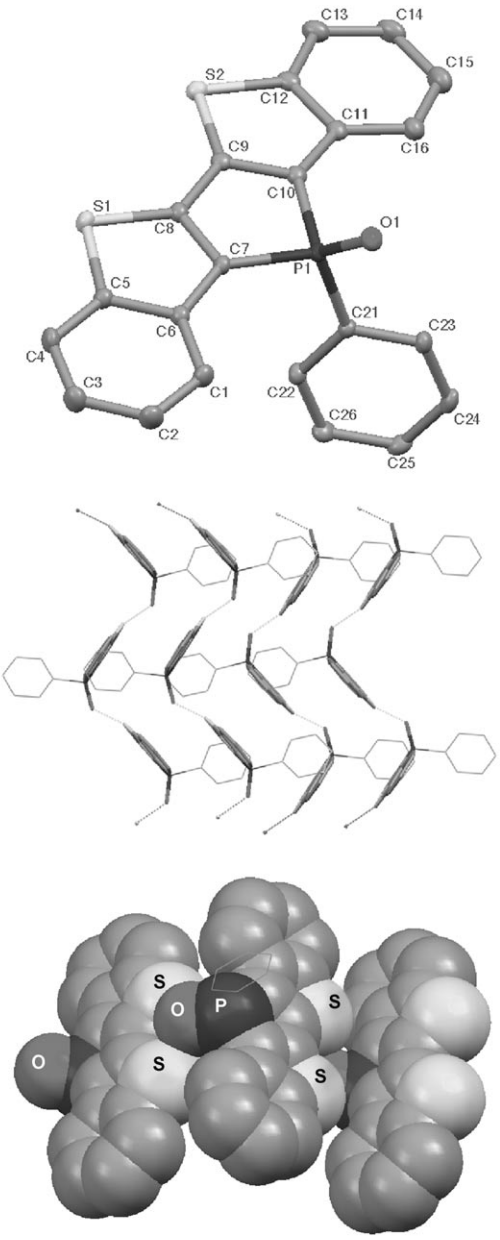

Figure 2. Top: Molecular structure of **4** in the solid state (50% probability level); hydrogen atoms are omitted for clarity. Selected bond lengths [Å] and angles [°]: P1−O1 1.4876(14), P1−C7 1.793(2), P1−C10 1.804(2), P1−C21 1.797(2), S1−C8 1.729(2), S1−C5 1.746(2), S2−C9 1.736(2), S2−C12 1.745(2), C1−C2 1.381(3), C2−C3 1.411(3), C1−C6 1.407(3), C3−C4 1.383(3), C4−C5 1.393(3), C5−C6 1.416(3), C6−C7 1.429(3), C7−C8 1.381(3), C8−C9 1.475(3), C9−C10 1.375(3), C10−C11 1.429(3), C11−C12 1.411(3), C12−C13 1.404(3), C13−C14 1.380(3), C14−C15 1.409(3), C15−C16 1.379(3), C11−C16 1.409(3); O1-P1-C7 118.47(9), O1-P1-C21 110.97(8), C7-P1-C21 108.93(9), O1-P1-C10 116.98(9), C7-P1-C10 91.70(9), C21-P1-C10 108.07(9). Middle: Molecular packing of **4**. Bottom: Space-filling representation of the O···S interactions between neighboring molecules in the structure of **4** (H atoms omitted for clarity).

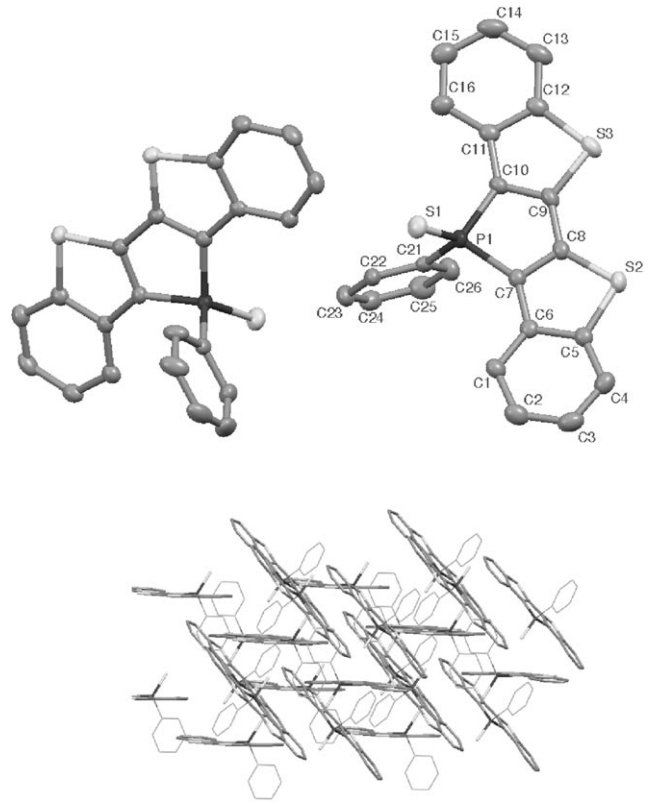

Figure 3. Top: Molecular structure of **5** in the solid state (50% probability level); hydrogen atoms are omitted for clarity; selected bond lengths [Å] and angles [°]: P1−S1 1.9427(11), P1−C10 1.809(3), P1−C7 1.811(3), P1−C21 1.824(3), S2−C8 1.728(3), S2−C5 1.759(3), S3−C9 1.731(3), S3−C12 1.749(3), C1−C2 1.376(4), C1−C6 1.406(4), C2−C3 1.407(4), C3−C4 1.384(4), C4−C5 1.387(4), C5−C6 1.420(4), C6−C7 1.431(4), C7−C8 1.376(4), C8−C9 1.454(4), C9−C10 1.366(4), C10−C11 1.433(4), C11−C12 1.423(4), C12−C13 1.402(4), C13−C14 1.383(5), C14−C15 1.412(5), C15−C16 1.374(4), C11−C16 1.409(4); C10-P1-C7 91.28(14), C10-P1-C21 107.03(13), C7-P1-C21 107.70(13), C10-P1-S1 117.08(10), C7-P1-S1 116.55(10), C21-P1-S1 114.56(10), C8-S2-C5 90.42(14), C9-S3-C12 90.13(15). Bottom: Molecular packing of **5**.

Cationic phospholium species **8** was obtained as single crystals from a concentrated solution of **8** in acetone at room temperature and has a single molecule in the unit cell (Figure 4, top). Compared to the oxidized and sulfurized compounds **4** and **5**, the P−C bonds in **8** are significantly shorter due to the cationic nature of the phosphorus center. The P−Me bond length of 1.763(3) Å is somewhat shorter than that of the few other structurally characterized phospholium salts (1.775(3)–1.787(5) Å).[32] The bond lengths in the dithienophosphole subunit are comparable to those in phospholium salt **B** (R = Ph; R′ = H, E = Me^+).[24d] Again, the slight differences can be explained by the more extended π system consisting of five rings. It is worth noting that the ion pair of **8** is well separated in the solid state. Although the arrangement of **8** in the solid state (Figure 4, bottom) shows only weak interactions between the benzannelated dithieno scaffold of neighboring molecules, distances of 3.6 Å indicate that π-stacking interactions are present here as well.

These very different solid-state structures of the three relatives of the same heteropentacene dithienophosphole family nicely illustrate how the versatile reactivity of the phosphorus center can efficiently be utilized to tune the or-

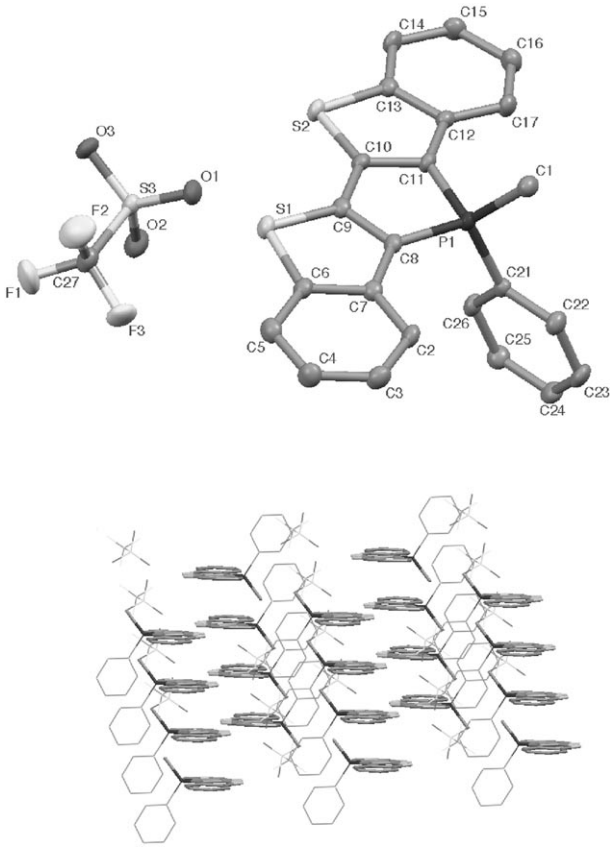

Figure 4. Top: Molecular structure of **8** in the solid state; hydrogen atoms are omitted for clarity (probability level 50%); selected bond lengths [Å]: P1–C1 1.763(3), P1–C8 1.777(2), P1–C11 1.773(2), P1–C21 1.783(2), S1–C6 1.753(1), S1–C9 1.712(1), S2–C10 1.715(1), S2–C13 1.745(1), C2–C3 1.367(4), C2–C7 1.395(3), C3–C4 1.396(4), C4–C5 1.381(4), C5–C6 1.387(3), C6–C7 1.412(3), C7–C8 1.422(3), C8–C9 1.370(3), C9–C10 1.456(3), C10–C11 1.369(3), C11–C12 1.422(3), C12–C13 1.410(3), C12–C17 1.399(3), C13–C14 1.384(3), C14–C15 1.376(3). Bottom: Molecular packing of **8**.

ganization in the solid state. Even the simplest variations, such as replacing an oxygen atom with sulfur, have tremendous impact on the packing motif and possibly on the performance of corresponding OFET devices.

Electrochemical properties: Although organic semiconductors should intrinsically be able to conduct charge either through their valence band (p-channel) or their conduction band (n-channel), that is, they should show ambipolar behavior, in many materials the p-channel dominates.[1b] However, it is much more desirable to generate n-channel (or n-type) materials, as this conduction mechanism is more efficient in devices.[1] Much effort has therefore been dedicated to the development of new organic n-type semiconductors.[1,2] As already indicated by the fluorescence properties of the various members of this dithienophosphole family, modification of the phosphorus center also has a significant impact on the electronic structure. Increasing the acceptor character of the phosphorus center significantly affects the LUMO energy level,[15,17] which is already fairly low in phospholes to begin with. In general, the electron affinity of molecules with heavier elements is higher than that of their carbon analogues. For example, a P=C bond is very effective in this respect: triphosphabenzene has a high electron affinity, while that of benzene is negative (it repels electrons).[33] Naphthalene is a better electron acceptor than benzene; its electron affinity is -0.2 eV (≈ 0).[34] Thus, larger π systems are also better electron acceptors, and with increasing number of phosphorus atoms in the system the stability of the anion further increases. These features led us to investigate the electrochemical behavior of the heteropentacene dithienophospholes, in order to determine their preferred conduction channel. Our recent studies suggested that dithienophospholes may be good candidates for ambipolar semiconductors, or may even show dominant n-channel behavior.[22,24]

For the electrochemical studies, we chose trivalent phosphole **3**, oxidized/sulfurized species **4**/**5**, and phospholium cation **8** as a representative set of compounds. We found that the electrochemical behavior strongly depends on the nature of the central phosphorus atom (Table 2). Trivalent

Table 2. Cyclovoltammetric data ($E_{1/2}$ vs. Ag/AgCl) for **3**, **4**, and **8**.

	E_{ox} [V]	E_{red} [V]	ΔE [V]
3[a]	1.42[c]	−1.95[d]	3.37
4[b]	1.61[c]	−1.45[e]	3.06
8[b]	–	−1.25[d]	–

[a] In THF. [b] In CH_2Cl_2. [c] Irreversible. [d] Quasireversible. [e] Reversible (reduction peak separation ca. 60 mV).

phosphole **3** indeed shows ambipolar behavior with an irreversible oxidation at $E_{ox} = 1.42$ V (vs. $Ag^+/AgCl$) that is shifted somewhat from that of the parent system ($E_{ox} = 1.20$ V vs. SCE),[22b] but more importantly also shows a quasireversible reduction at $E_{red} = -1.95$ V, consistent with strong electron affinity in this heteropentacene. Oxidation of the phosphorus center in **4** significantly affects the redox properties of the system. Phosphole oxide **4** still shows some ambipolar behavior, but reduction is significantly more dominant in this material. Due to the increased electron-acceptor character of the phosphorus center, oxidation (irreversible) is disfavored, as is evident in the further shift of the oxidation potential ($E_{ox} = 1.61$ V) compared to the parent dithienophosphole **B** (R = Ph, R′ = H, E = lone pair)[22b] and phosphole **3**. Reduction in **4** is ideally reversible at $E_{red} = -1.45$ V, consistent with increased electron affinity and a very stable radical anion (Figure 5). Unfortunately, the electrochemistry of the sulfurized species **5** could not be determined under the conditions available to us. Studies at scan rates of 100 and 500 mV s^{-1} revealed that, likely due to the presence of the thio group at phosphorus, **5** was irreversibly adsorbed on the Pt electrode used for these studies and that this process was rather slow. Neither oxidation nor reduction potentials could be obtained. However, judging from the photophysical properties of **5**, as well as from theoretical investigations, it can be assumed that the

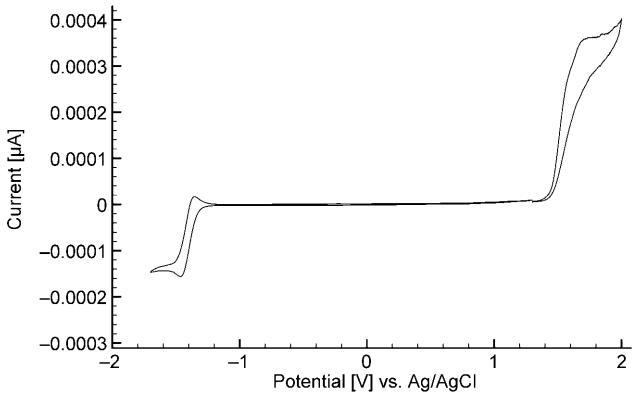

Figure 5. Cyclic voltammogram of **4** at 293 K. Conditions: Pt wire as working electrode; solution (ca. 0.1 mM) in CH_2Cl_2 with NBu_4PF_6 as supporting electrolyte; scan rate 100 mV s^{-1}; potentials are referred to an Ag/AgCl/KCl 3 M electrode.

redox properties are likely similar to those of oxide **4**. Methylated phospholium compound **8** could be investigated without further complications. Its even stronger electron-acceptor character, due to the presences of a cationic charge, exclusively leads to characteristics necessary for n-type behavior; an oxidation process cannot be observed within the available window ($E \leq 2.0$ V), and the reduction process is strongly favored ($E_{red} = -1.25$ V). We found reduction to be rather slow. Investigation of the reduction potential of **8** at different scan rates (10, 100, and 500 mV s^{-1}) showed no true reversibility; that is, the process is kinetically controlled and quasireversible.[35] Notably, the preferred one-electron reduction of a series of related phospholium compounds was recently reported by Le Floch and co-workers,[32] who showed that reduction of these cationic species provides very stable neutral radicals. The values observed for **3**, **4**, and **8** are also lower than those recently reported by Matano et al. for somewhat related bithiophene-fused benzo[*c*]phospholes.[36]

The electrochemical studies on heteropentacenes **3**, **4**, and **8** nicely show that the versatile reactivity of phosphorus can also be used to effectively manipulate the electronic properties of the materials. More importantly, the presence of the phosphorus center intrinsically gives rise to features important for n-channel materials that can be easily tuned by means of simple modifications.

Theoretical calculations: The B3LYP/6-31G* optimized structures are similar to those obtained by X-ray crystallography. In the case of **4**, however, the phenyl group was optimized to be in the mirror plane of the molecule, while the X-ray structure of the molecule is asymmetric. Apparently the interaction between molecules in the unit cell makes the asymmetric arrangement favorable; the potential-energy surface for rotation about P–C bond in the gas phase proved to be quite flat. Interestingly, the computed TD spectra of the two structures are similar (406 and 326 nm vs. 405 and 324 nm are predicted for the first two bands for the X-ray and computed structures, respectively), that is, rotation of the phenyl group about the P–C bond has a small effect on the photophysical properties of the system. The computed TD spectra are in good agreement with the measured absorption maxima in solution (Table 1).

To investigate the S···O(=P) interactions in more detail, a dimer of **4** was also optimized. At the B3LYP/3-21G* level the dimer has a structure similar to that found by X-ray diffraction with S···O distances of 2.820 and 2.818 Å and rotation of the phenyl substituent at phosphorus from the symmetrical position. At the B3LYP/6-31G* level, however, the S···O distance increased to 3.272 and 3.222 Å. Similar distances were obtained for the dimer of **B** (R = Ph, R′ = H, E = O). The B3LYP/6-31G*//B3LYP/3-21G(*) electron density, analyzed by the atoms in molecules (AIM) method of Bader,[37] revealed two bond critical points, each between the O and one of the two S atoms of the neighboring molecule with an electron density of 0.015. Similar electron densities were reported for bond critical points in molecular assemblies with S···O interactions.[31d,e] A ring critical point was located for the –S–C=C–S–O fragment. The dimer was more stable than two monomers by 2.1 kcal mol^{-1} (uncorrected for basis-set superposition error). To analyze the effect of this interaction on the photophysical properties, TDDFT calculations at the B3LYP/6-31G*//B3LYP/3-21G(*) level were carried out on the dimer of **4**. The computed transition energy of the dimer of 509.9 nm (albeit with low intensity) contrasts with the value of 406 nm (Table 1) obtained for monomeric **4**. This significant shift is in accordance with the observed difference between the solution and crystal-phase absorption spectra (Table 1).

We also investigated the redox properties of **3**–**5** and **8** by means of theoretical calculations. Thus, we calculated ionization energies of **3**–**5** and the electron-attachment energies of **3**–**5** and **8** by optimizing the radical anion and cation. These calculations were carried out at the B3LYP/6-31+G* level of theory, which was shown to give reliable values for anions that have electron affinities more positive than about −1 eV.[33] In each case the electron affinity of the molecules is positive, and thus a stable anion is formed. The computed ionization energies and electron affinities are compiled in Table 3. From the data it is evident that the electron affinities are larger for molecules with more extended π delocali-

Table 3. B3LYP/6-31+G* adiabatic ionization energies (aIE) [kcal mol^{-1}], electron affinities (aEA) [kcal mol^{-1}], and Kohn–Sham HOMO and LUMO energies [eV] of **3**–**5**, **8** and related derivatives of **B**.

	aIE	aEA	Δ(IE,EA)	HOMO	LUMO
B (R′ = H, R = Ph, E = lp[a])	162.1	8.1	154.0	−5.67	−1.62
B (R′ = H, R = Ph, E = O)	170.1	20.2	149.9	−6.03	−2.15
B (R′ = H, R = Ph, E = S)	168.3	21.8	146.5	−5.98	−2.16
B$^+$ (R′ = H, R = Ph, E = Me)	–	101.7	–	−9.44	−5.66
3	155.6	19.9	135.7	−5.60	−1.95
4	161.4	30.3	131.1	−5.85	−2.39
5	164.5	32.5	132.0	−5.88	−2.44
8[b]	–	105.8	–	−8.94	−5.66

[a] lp = lone pair. [b] Cation part only.

zation (**3**–**5** and **8** have larger electron affinities than the corresponding **B**-type compounds). The largest electron affinity is exhibited by cationic species **8**. The *P*-oxide and *P*-sulfide also have slightly higher electron affinity than their parent phosphole. All these findings are in agreement with the reduction potentials observed for these compounds, that is, **4**, **5**, and especially **8** are good candidates for exhibiting n-type behavior. To investigate the effect of other heteroatoms on the electron-acceptor properties, we also computed the redox properties of the arsenic analogues of **3** and **8**. The As compounds exhibit similar redox properties to their phosphorus analogues, and hence no further improvement of the n-type conductivity can be expected by replacing phosphorus with its heavier analogue.

Conclusion

We have synthesized a series of phosphorus-based heteropentacenes by simple chemical modifications at the trivalent phosphorus center. This signature of organophosphorus π-conjugated materials allows a whole family of derivatives to be generated from just one precursor material. Chemical modification of the central phosphorus atom provides materials with significantly altered properties, including organization in the solid state, photoluminescence, and redox behavior, all of which are of fundamental importance for organic semiconductors. Even the simplest variations, such as replacing an oxygen atom by a sulfur atom at the phosphorus center, have tremendous impact on the solid-state packing of the compounds, particularly the phosphole oxide, which shows an intriguing intermolecular S···O interaction that may improve the charge carrier mobility of the materials in devices. Furthermore, intense photoluminescence of the pentacene-analogous dithienophospholes in the solid state suggests potential application as active materials in light-emitting field-effect transistors (LEFETs). Most importantly, theoretical and electrochemical studies on representative members of this family revealed that the phosphorus atom intrinsically furnishes the materials with features important for n-channel (or n-type) or ambipolar semiconductor behavior, which can again be efficiently manipulated by means of the electronic nature of the phosphorus center. Our electrochemical studies showed that phosphole oxide **4** exhibits the best reversible reduction, whereas cationic phospholium species **8** has the lowest reduction potential. These observations suggest that both materials may be excellent candidates for n-type semiconductors. Studies on implementation of **4** into an OFET device are underway and will also be extended to the other members of this heteropentacene family.

Experimental Section

General procedures: Reactions were carried out in dry glassware under an inert atmosphere of purified argon or nitrogen by using Schlenk techniques. Solvents were dried over appropriate drying agents and then distilled. $CuCl_2$, *n*BuLi (2.5 M in hexane), H_2O_2 (30% in H_2O), sulfur, $BH_3{\cdot}SMe_2$ (1 M in CH_2Cl_2), and methyl triflate were used as received. *N*,*N*,*N*,*N*-Tetramethylethylenediamine (TMEDA) and phenyldichlorophosphane were distilled prior to use. 2,3-Dibromobenzo[*b*]thiophene[38] and [Au(tht)Cl][39] were prepared by literature methods. ^{1}H NMR, ^{13}C{^{1}H} NMR, ^{31}P{^{1}H} NMR, and ^{11}B NMR spectra were recorded on a Bruker DRX 400, Varian Mercury 200, or Unity 500 MHz spectrometer. Chemical shifts were referenced to external 85% H_3PO_4 (^{31}P), $BF_3{\cdot}Et_2O$ (^{11}B), or TMS (^{13}C, ^{1}H). Elemental analyses were performed at the Microanalytical Laboratory of the Institut für Anorganische und Analytische Chemie, Johannes Gutenberg-Universität, Mainz; the Institut für Organische Chemie, RWTH-Aachen University; and the Department of Chemistry at the University of Calgary. Crystal data and details of data collection are provided in Table 4. Diffraction data for **4**, **5**, and **8** were collected on a Bruker SMART D8 goniometer with APEX CCD detector by using graphite-monochromated $Mo_{K\alpha}$ radiation ($\lambda = 0.71073$ Å). The structures were solved by direct methods (SHELXTL) and refined on F^2 by full-matrix least-squares techniques. Hydrogen atoms were included by using a riding model. EI mass spectra were recorded on a Finigan SSQ 7000 spectrometer. Fluorescence spectra were recorded on a JASCO FP6500 spectrofluorometer; for the solid-state measurements, a polycrystalline sample was placed in the corresponding solid-state accessory. Electrochemical studies were performed on an Autolab PGSTAT302 instrument with a Pt wire electrode (flamed in a torch) as working electrode, Pt mesh as counterelectrode, and an Ag/AgCl/KCl 3 M reference electrode; supporting electrolyte was NBu_4PF_6; standard scan rates were 100 mV s^{-1} for **4**, **5**, and **8** and 200 mV s^{-1} for **3**.

Synthesis of 2: 2,3-Dibromobenzo[*b*]thiophene (**1**, 20 mmol, 5.84 g) was dissolved in diethyl ether (250 mL) and *n*BuLi (21 mmol, 8.4 mL) was added at −78 °C. The reaction mixture was stirred for 20 min at this temperature, then for 1 h at −20 °C, during which a yellow suspension was obtained. After cooling to −78 °C, $CuCl_2$ (30 mmol, 4 g) was added and the reaction mixture was allowed to warm to room temperature and was further stirred at this temperature for 10 h. The brown precipitate was filtered off and HCl (5 N, 300 mL) was added at 0 °C. The product was extracted with $CHCl_3$ and diethyl ether, and the red organic phase was washed with HCl (5 N) and H_2O and dried with $MgSO_4$. After evaporating all volatile materials the crude product was obtained as dark oil. The pure product could be obtained as a pink-tinted solid after washing with acetone. Needle-shaped crystals of **2** could be obtained by crystallization from pentane (2.31 g, 54.5% yield). ^{1}H NMR (200 MHz, $CDCl_3$): $\delta =$ 7.95–7.78 (m, 4H), 7.40–7.55 ppm (m, 4H); ^{13}C{^{1}H} NMR (125 MHz, $CDCl_3$): $\delta = 139.1$, 137.94, 129.34, 126.30 (s; benz), 125.42 (s; benz), 123.99 (s; benz), 122.23 (s; benz), 110.83 ppm (s; ArBr).

Synthesis of 3: *n*BuLi (2.83 mL, 7.08 mmol) was added dropwise to a solution of **2** (1.80 g, 2 mmol) and TMEDA (2 mL, 10 mmol) in diethyl ether (200 mL) at −78 °C. After stirring for 10 min, $PhPCl_2$ (0.63 g, 3.54 mmol) was added and the resulting suspension was allowed to warm quickly to room temperature. The solvent was then removed under vacuum, and the residue taken up in CH_2Cl_2 (100 mL) and filtered through neutral alumina. After evaporation of the solvent the residue was washed with pentane and diethyl ether to give **3** as light yellow powder (yield 72%). ^{31}P{^{1}H} NMR (80.9 MHz, $CDCl_3$): $\delta = -25.1$ ppm (s); ^{1}H NMR (200 MHz, $CDCl_3$): $\delta =$ 7.91–7.84 (br, 2H) 7.76–7.68 (br, 2H), 7.48–7.40 (br, 3H) 7.36–7.24 ppm (br, 6H); ^{13}C{^{1}H} NMR (100 MHz, $CDCl_3$): $\delta = 143.7$ (d, ^3J(C,P) = 4.8 Hz; Ar), 143.1 (d, ^3J(C,P) = 9.58 Hz; Ar), 142.3 (d, ^4J(C,P) = 3.4 Hz; *p*-Ph), 138.3 (d, ^1J(C,P) = 17.3 Hz; *ipso*-Ar), 133.5 (d, ^2J(C,P) = 21.1 Hz; *o*-Ph), 132.2 (d, ^2J(C,P) = 13.4 Hz, *o*-Ph), 130.3 (s) 129.5 (d, ^3J(C,P) = 7.7 Hz; *m*-Ph), 125.7 (s; benzo), 124.9 (s; benzo), 124.1 (s; benzo), 122.5 ppm (s; benzo); MS (70 eV, EI): *m*/*z* (%): 372 (100) [M^+], 340 (70) [$M^+ - S$], 295 (40) [$M^+ - Ph$]; HRMS calcd for $C_{22}H_{13}PS_2$ [M^+]: 372.0196; found: 372.0180; elemental analysis calcd (%) for $C_{22}H_{13}PS_2{\cdot}0.5\,LiCl/Et_2O$ (430.70 g mol^{-1}): C 66.93, H 4.21; found: C 67.27, H 4.35.

Synthesis of 4: Phosphole **3** (60 mg, 0.16 mmol) was dissolved in CH_2Cl_2 (25 mL), an excess of H_2O_2 (2 mL, 30% aqueous solution) was added, and the mixture was then stirred for 2 h at room temperature. After

Table 4. Crystal data and structure refinement for **4**, **5**, and **8**.[a]

	4	**5**	**8**
formula	$C_{22}H_{13}OPS_2$	$C_{22}H_{13}SPS_2$	$C_{24}H_{16}F_3OPS_3$
M_r	388.41	404.47	536.52
T [K]	153(2)	110(2)	130(2)
λ [Å]	0.71073	0.71073	0.71073
crystal system	monoclinic	triclinic	triclinic
space group	$P2_1/n$	$P\bar{1}$	$P\bar{1}$
a [Å]	11.151(2)	8.292(2)	9.3146(13)
b [Å]	10.998(2)	13.855(3)	10.6391(15)
c [Å]	15.705(3)	17.940(4)	12.5703(18)
α [°]	90	110.977(5)	113.546(2)
β [°]	93.90(3)	91.980(5)	93.590(2)
γ [°]	90	103.165(5)	93.141(2)
V [Å^3]	1749.2(6)	1858.5(7)	1135.4(3)
Z	4	4	2
ρ_{calcd} [Mg m^{-3}]	1.475	1.446	1.569
μ [mm^{-1}]	0.404	0.488	0.448
$F(000)$	800	832	548
crystal size [mm]	$0.47\times0.24\times0.06$	$0.24\times0.20\times0.09$	$0.28\times0.18\times0.09$
θ range [°]	2.26–30.12	1.23–27.17	1.77–25.65
index ranges	$-14\le h\le13$	$-10\le h\le10$	$-11\le h\le11$
	$-15\le k\le15$	$-17\le k\le17$	$-12\le k\le12$
	$-22\le l\le21$	$-22\ l\le22$	$-15\le l\le15$
reflections collected	22115	23875	12527
independent reflections	5038 (R(int) = 0.0508)	8210 (R(int) = 0.0564)	4292 (R(int) = 0.0520)
completeness to θ [°]	30.12 (97.6%)	27.17 (99.4%)	25.65 (99.7%)
absorption correction	empirical	empirical	empirical
max/min transmission	0.9762/0.8327	0.9574/0.89191	0.9608/0.8848
data/restraints/parameters	5038/0/235	82102/0/469	4292/0/371
GoF on F^2	1.139	0.932	0.931
final R indices [$I>2\sigma(I)$]	$R_1=0.0520$, $wR_2=0.1148$	$R_1=0.0433$, $wR_2=0.0864$	$R_1=0.0370$, $wR_2=0.0739$
R indices (all data)	$R_1=0.0632$, $wR_2=0.1195$	$R_1=0.0654$, $wR_2=0.1123$	$R_1=0.0550$, $wR_2=0.0789$
largest diff. peak/hole [e Å^3]	0.575/−0.331	0.530/−0.311	0.368/−0.328

[a] CCDC-693332 (**4**), CCDC-693333 (**5**) and CCDC-693334 (**8**) contain the supplementary crystallographic data for this paper. These data can be obtained free of charge from The Cambridge Crystallographic Data Centre via www.ccdc.cam.ac.uk/data_request/cif.

quenching with water, the organic layer was separated and dried with $MgSO_4$, and all volatile materials were removed in vacuum. The product **4** was obtained as a light yellow solid and could be recrystallized from acetone to give needle-shaped crystals (53 mg, 84% yield). $^{31}P\{^1H\}$ NMR (80.9 MHz, $CDCl_3$): $\delta=-16.7$ ppm; ^1H NMR (200 MHz, $CDCl_3$): $\delta=$ 7.92–7.76 (m, 6H; Ar) 7.55–7.23 ppm (m, 7H; Ar); $^{13}C\{^1H\}$ NMR (100 MHz, $CDCl_3$): $\delta=146.7$ (d, ^2J(C,P) = 23.4 Hz; Ar), 143.4 (d, ^3J-(C,P) = 13.4 Hz; Ar), 136.1 (d, ^3J(C,P) = 13.4 Hz; Ar), 133.9 (d, ^1J(C,P) = 111.2 Hz; *ipso*-Ar), 132.5 (d, ^3J(C,P) = 2.9 Hz; benzo), 130.2 (d, ^2J(C,P) = 11.5 Hz, *o*-Ph), 129.2 (d, ^3J(C,P) = 12.5 Hz; *m*-Ph), 126.3 (s; *p*-Ph), 125.3 (s; benzo), 123.5 (s; benzo), 123.1 (s; benzo), 121.8 ppm (d, J(C,P) = 96.8 Hz, *ipso*-Ph); elemental analysis calcd (%) for $C_{22}H_{13}OPS_2$ (388.44 g mol^{-1}): C 68.02, H 3.37, S 16.51; found: C 68.68, H 2.80, S 16.98.

Synthesis of 5: Phosphole **3** (93 mg, 0.25 mmol) was dissolved in CH_2Cl_2 (30 mL) and sulfur (excess) was added. The mixture was stirred at room temperature for 5 h until no further shift of the fluorescence could be observed. All volatile materials were removed in vacuo. The product **5** was obtained as a light yellow solid. The residue was taken up in *n*-pentane, from a concentrated solution in which crystals formed (73 mg, 73% yield). $^{31}P\{^1H\}$ NMR (80.9 MHz, $CDCl_3$): $\delta=23.1$ ppm (s); ^1H NMR (200 MHz, $CDCl_3$): $\delta=$ 7.97–7.78 (m, 6H; Ar) 7.55–7.30 ppm (m, 7H; Ar); $^{13}C\{^1H\}$ NMR (100 MHz, $CDCl_3$): $\delta=145.1$ (d, ^2J(C,P) = 20.1 Hz; Ar), 143.4 (d,^3J(C,P) = 13.4 Hz; Ar), 135.7 (d, ^1J(C,P) = 92.9 Hz; *ipso*-Ar), 135.5 (d, ^3J(C,P) = 13.4 Hz; Ar), 132.5 (d, ^3J(C,P) = 3.9 Hz; benzo), 130.6 (d, ^2J(C,P) = 12.5 Hz, *o*-Ph), 129.1 (d, ^3J(C,P) = 13.4 Hz; *m*-Ph), 126.3 (s; *p*-Ph), 125.4 (s; benzo), 123.6 (s; benzo), 1232.5 (s; benzo), 123.3 ppm (d, ^1J(C,P) = 52.7 Hz, *ipso*-Ph); elemental analysis calcd (%) for $C_{22}H_{13}S_3P$ (403.99 g mol^{-1}): C 65.32, H 3.24, S 23.78; found: C 65.09, H 3.53, S 23.42.

Synthesis of 6: An excess of $BH_3{\cdot}SMe_2$ (2 mL, 1 M in CH_2Cl_2) was added to phosphole **3** (372 mg, 1 mmol) in CH_2Cl_2 (30 mL) and the mixture was stirred for 5 h at room temperature. After evaporation of the solvent the crude product could be obtained as a yellow powder, which was washed with *n*-pentane and recrystallized from toluene (243 mg, 63% yield). $^{31}P\{^1H\}$ NMR (80.9 MHz, $CDCl_3$): $\delta=$ 16.9 ppm (s); $^{11}B\{^1H\}$ NMR (160.3 MHz, $CDCl_3$): $\delta=-39.3$ ppm (brs; BH_3); ^1H NMR (200 MHz, $CDCl_3$): $\delta=$ 7.92–7.76 (m, 6H; Ar) 7.55–7.30 (m, 7H; Ar); 1.28 ppm (s, 3H, BH_3); $^{13}C\{^1H\}$ NMR (100 MHz, $CDCl_3$): $\delta=145.7$ (d, ^3J(C,P) = 10.2 Hz; Ar), 143.3 (d, ^3J(C,P) = 10.7 Hz; Ar), 136.4 (d, ^3J(C,P) = 14.4 Hz; Ar), 134.2 (d, ^1J(C,P) = 66.0 Hz; *ipso*-Ar), 133.1 (d, ^2J(C,P) = 21.5 Hz; *o*-Ph), 132.2 (d, ^4J(C,P) = 2.5 Hz; *p*-Ph), 132.04 (d, ^3J(C,P) = 11.1 Hz; *m*-Ph), 129.3 (d, ^3J(C,P) = 12.5 Hz; Ar), 126.1 (s; benzo), 125.4 (s; benzo), 123.7 (s; benzo), 122.7 ppm (s; benzo).

Synthesis of 7: [Au(tht)Cl] (320 mg, 1 mmol) was added to a solution of **3** (372 mg, 1 mmol) in CH_2Cl_2 (20 mL). After stirring for 2 h at room temperature, the yellow precipitate was filtered off, washed with *n*-pentane, and dried in vacuo (338 mg, 56% yield). $^{31}P\{^1H\}$ NMR (80 MHz, $CDCl_3$): $\delta=$ 2.44 ppm (s); ^1H NMR (200 MHz, $CDCl_3$): $\delta=$ 7.99–7.96 (m, 2H; Ar) 7.83–7.79 (m, 2H; Ar) 7.77–7.71 (m, 2H; Ar) 7.58–7.53 (m, 1H; Ar) 7.48–7.41 ppm (m, 6H; Ar); $^{13}C\{^1H\}$ NMR (100 MHz, $CDCl_3$): $\delta=143.4$ (d, ^3J(C,P) = 2.5 Hz; Ar), 135.8 (d, ^3J-(C,P) = 15.7 Hz; Ar), 133.6 (d, ^3J(C,P) = 18.9 Hz; Ar), 133.1 (d, ^4J(C,P) = 2.5 Hz; *p*-Ph), 129.8 (d, ^3J(C,P) = 13.1 Hz; *m*-Ph), 126.6 (s; benzo), 125.8 (s; benzo), 123.9 (s; benzo), 122.3 ppm (s; benzo).

Synthesis of 8: An excess of methyl triflate (200 mg, 1.2 mmol) was added to a solution of phosphole **3** (406 mg, 1.09 mmol) in CH_2Cl_2 (25 mL) and the mixture was stirred for 24 h at room temperature. The yellow suspension became dark orange. After evaporating all volatile materials in vacuo the remaining solid was washed with *n*-pentane, diethyl ether, and acetone. The product **8** was obtained as a yellow-orange solid. Recrystallization from acetone gave single crystals suitable for X-ray analysis (400 mg, 74% yield). $^{31}P\{^1H\}$ NMR (80.9 MHz, $CDCl_3$): $\delta=$ 11.4 ppm (s); ^1H NMR (200 MHz, $CDCl_3$): $\delta=$ 8.01 (m, 2H; Ar) 7.91 (m, 4H), 7.69 (m, 1H; *p*-Ph), 7.61 (m, 2H), 7.54 (2H), 7.45 (2H), 3.01 ppm (d, ^{3}J(P,H) 14.8 Hz; PMe); $^{13}C\{^1H\}$ NMR (100 MHz, $CDCl_3$): $\delta=150.6$ (d, ^2J(C,P) = 23.4 Hz; Ar), 143.5 (d,^2J(C,P) = 21.0 Hz; Ar), 141.6 (d, ^1J(C,P) = 58.3 Hz; *ipso*-Ar), 136.3 (d, ^4J(C,P) = 3.0 Hz; Ar), 134.6 (d, ^3J(C,P) = 14.2 Hz; benzo), 132.7 (d, ^2J(C,P) = 13.2 Hz, *o*-Ph), 131.3 (d, ^3J(C,P) = 14.2 Hz; *m*-Ph), 128.5 (s; *p*-Ph), 127.4 (s; benzo), 124.3 (s; benzo), 122.9 (s; benzo), 121.7 (d, ^1J(C,P) = 81.5 Hz, *ipso*-Ph), 122.8 (s; Ar), 122.0 (s; Ar), 6.9 ppm (d, ^1J(C,P) = 53.0 Hz; CH_3); elemental analysis calcd (%) for $C_{24}H_{16}F_3O_3PS_3$ (563.55 g mol^{-1}): C 53.72, H 3.01; found: C 53.80, H 3.24.

Calculations: Theoretical calculations were carried out at the B3LYP/6-31G* level[40] by using the Gaussian 03 suite of programs.[41] This level of

the theory has provided satisfactory results for phosphole–thiophene oligomers.[20c,22b,24e] The geometries were fully optimized, and calculation of second derivatives at the resulting structures revealed only positive eigenvalues of the Hessian matrix. The vertical excitation energies were calculated at the optimized structures (and in case of **4** also at the X-ray structure) by the time-dependent (TD) DFT method with the B3LYP functional and the 6-31G* basis set. Further calculations were carried out for **3–5** and the corresponding radical cations and radical anions at the B3LYP/6-31+G* level, to properly account for the anionic states.

Acknowledgements

We thank Prof. J. Okuda for his generous support of this work. Prof. U. Englert is acknowledged for his help with the X-ray data collection. Financial support of the Fonds der Chemischen Industrie, BMBF, Deutsche Forschungsgemeinschaft (DFG), Natural Sciences and Engineering Research Council (NSERC) of Canada, and from the Hungarian Scientific Research Fund (OTKA Grant No T 049258) is gratefully acknowledged. T.B. thanks Alberta Ingenuity for a New Faculty Award.

[1] a) A. R. Murphy, J. M. J. Fréchet, *Chem. Rev.* **2007**, *107*, 1066–1096; b) J. Zaumseil, H. Sirringhaus, *Chem. Rev.* **2007**, *107*, 1296–1323; c) S. Allard, M. Forster, B. Souharce, H. Thiem, U. Scherf, *Angew. Chem.* **2008**, *120*, 4138–4167; *Angew. Chem. Int. Ed.* **2008**, *47*, 4070–4098; d) B. S. Ong, Y. Wu, Y. Li, P. Liu, H. Pan, *Chem. Eur. J.* **2008**, *14*, 4766–4778; e) H. E. Katz, Z. Bao, S. L. Gilat, *Acc. Chem. Res.* **2001**, *34*, 359–369; f) C. D. Dimitrakopoulos, P. R. L. Malenfant, *Adv. Mater.* **2002**, *14*, 99–117.

[2] a) J. E. Anthony, *Chem. Rev.* **2006**, *106*, 5028–5048; b) J. E. Anthony, *Angew. Chem.* **2008**, *120*, 460–492; *Angew. Chem. Int. Ed.* **2008**, *47*, 452–483.

[3] *Organic Light Emitting Devices* (Eds.: K. Müllen, U. Scherf), Wiley-VCH, Weinheim, **2006**.

[4] a) A. Kraft, A. C. Grimsdale, A. B. Holmes, *Angew. Chem.* **1998**, *110*, 416–443; *Angew. Chem. Int. Ed.* **1998**, *37*, 402–428; b) B. W. D'Andrade, S. R. Forrest, *Adv. Mater.* **2004**, *16*, 1585–1595; c) I. F. Perepichka, D. F. Perepichka, H. Meng, F. Wudl, *Adv. Mater.* **2005**, *17*, 2281–2305.

[5] a) G. A. Chamberlain, *Solar Cells* **1983**, *8*, 47–83; b) P. Peumans, A. Yakimov, S. R. Forrest, *J. Appl. Phys.* **2003**, *93*, 3693–3723; c) F. Padinger, R. S. Rittberger, N. S. Sariciftci, *Adv. Funct. Mater.* **2003**, *13*, 85–88; d) M. Svensson, F. L. Zhang, S. C. Veenstra, W. J. H. Verhees, J. C. Hummelen, J. M. Kroon, O. Inganaes, M. R. Andersson, *Adv. Mater.* **2003**, *15*, 988–991; e) B. C. Thompson, J. M. J. Fréchet, *Angew. Chem.* **2008**, *120*, 62–82; *Angew. Chem. Int. Ed.* **2008**, *47*, 58–77; f) S. Günes, H. Neugebauer, N. S. Sariciftci, *Chem. Rev.* **2007**, *107*, 1324–1338.

[6] a) *Handbook of Conducting Polymers*, 3rd ed. (Eds.: T. A. Skotheim, J. R. Reynolds), CRC Press, Boca Raton, **2007**; b) S. W. Thomas, III, G. D. Joly, T. M. Swager, *Chem. Rev.* **2007**, *107*, 1339–1386; c) D. T. McQuade, A. E. Pullen, T. M. Swager, *Chem. Rev.* **2000**, *100*, 2537–2574.

[7] a) J. A. Rogers, Z. Bao, M. Meier, A. Dodabalapur, O. J. A. Schueller, G. M. Whitesides, *Synth. Met.* **2000**, *115*, 5–11; b) J. A. Rogers, Z. Bao, K. Baldwin, A. Dodabalapur, B. Crone, V. R. Raju, V. Kuck, H. Katz, K. Amundson, J. Ewing, P. Drzaic, *Proc. Natl. Acad. Sci. USA* **2001**, *98*, 4835–4840; c) H. Sirringhaus, T. Kawase, R. H. Friend, T. Shimoda, M. Inbasekaran, W. Wu, E. P. Woo, *Science* **2000**, *290*, 2123–2126; d) S. P. Speakman, G. G. Rozenburg, K. J. Clay, W. I. Milne, A. Ille, I. A. Gardner, E. Bresler, J. H. G. Steinke, *Org. Electron.* **2001**, *2*, 65–73.

[8] a) J. Roncali, *Chem. Rev.* **1997**, *97*, 173–206; b) J. Roncali, *Macromol. Rapid Commun.* **2007**, *28*, 1761–1775.

[9] a) Q. Miao, X. Chi, S. Xiao, R. Zeis, M. Lefenfeld, T. Siegrist, M. L. Steigerwald, C. Nuckolls, *J. Am. Chem. Soc.* **2006**, *128*, 1340–1345; b) J. E. Anthony, D. L. Eaton, S. R. Parkin, *Org. Lett.* **2002**, *4*, 15–18; c) K. Walzer, B. Maennig, M. Pfeiffer, K. Leo, *Chem. Rev.* **2007**, *107*, 1233–1271.

[10] a) Y. Shirota, H. Kageyama, *Chem. Rev.* **2007**, *107*, 953–1010; b) V. Coropceanu, J. Cornil, D. A. da Silva Filho, Y. Olivier, R. Sibey, J.-L. Brédas, *Chem. Rev.* **2007**, *107*, 926–952; c) M. D. Curtis, J. Cao, J. W. Kampf, *J. Am. Chem. Soc.* **2004**, *126*, 4318–4328; d) T. M. Pappenfus, R. J. Chesterfield, C. D. Frisbie, K. R. Mann, J. Casado, J. D. Raff, L. L. Miller, *J. Am. Chem. Soc.* **2002**, *124*, 4184–4185; e) R. J. Chesterfield, C. R. Newman, T. M. Pappenfus, P. C. Ewbank, M. H. Haukaas, K. R. Mann, L. L. Miller, C. D. Frisbie, *Adv. Mater.* **2003**, *15*, 1278–1282; f) T. M. Pappenfus, J. D. Raff, E. J. Hukkanen, J. R. Burney, J. Casado, S. M. Drew, L. L. Miller, K. R. Mann, *J. Org. Chem.* **2002**, *67*, 6015–6024; g) X. C. Li, H. Sirringhaus, F. Garnier, A. B. Holmes, S. C. Moratti, N. Feeder, W. Clegg, S. J. Teat, R. H. Friend, *J. Am. Chem. Soc.* **1998**, *120*, 2206–2207.

[11] K. Xiao, Y. Liu, T. Qi, W. Zhang, F. Wang, J. Gao, W. Qiu, Y. Ma, G. Cui, S. Chen, X. Zhan, G. Yu, J. Qin, W. Hu, D. Zhu, *J. Am. Chem. Soc.* **2005**, *127*, 13281–13286.

[12] M. L. Tang, T. Okamoto, Z. Bao, *J. Am. Chem. Soc.* **2006**, *128*, 16002–16003.

[13] J. G. Laquindanum, H. E. Katz, A. J. Lovinger, *J. Am. Chem. Soc.* **1998**, *120*, 664–672.

[14] J. Gao, R. Li, L. Li, Q. Meng, H. Jiang, H. Li, W. Hu, *Adv. Mater.* **2007**, *19*, 3008–3011.

[15] T. Baumgartner, R. Réau, *Chem. Rev.* **2006**, *106*, 4681–4727 (correction: T. Baumgartner, R. Réau, *Chem. Rev.* **2007**, *107*, 303).

[16] a) D. Delaere, M. T. Nguyen, L. G. Vanquickenborne, *J. Phys. Chem. A* **2003**, *107*, 838–846; b) J. Ma, S. Li, Y. Jiang, *Macromolecules*, **2002**, *35*, 1109–1115; c) L. Nyulászi, *J. Phys. Chem.* **1995**, *99*, 586–591; d) L. Nyulászi, *Chem. Rev.* **2001**, *101*, 1229–1246; e) F. Mathey, *Chem. Rev.* **1988**, *88*, 429–453.

[17] a) W. Schäfer, A. Schweig, F. Mathey, *J. Am. Chem. Soc.* **1976**, *98*, 407–414; b) E. Mattmann, F. Mathey, A. Sevin, G. Frison, *J. Org. Chem.* **2002**, *67*, 1208–1213; c) E. Mattmann, F. Mercier, L. Ricard, F. Mathey, *J. Org. Chem.* **2002**, *67*, 5422–5425; d) L. Nyulászi, O. Holloczki, C. Lescop, M. Hissler, R. Réau, *Org. Biomol. Chem.* **2006**, *4*, 996–998; e) D. Delaere, P.-T. Nguyen-Nguyen, M. T. Nguyen, *Chem. Phys. Lett.* **2004**, *383*, 138–142; f) E. Mattmann, D. Simonutti, L. Ricard, F. Mercier, F. Mathey, *J. Org. Chem.* **2001**, *66*, 755–758.

[18] a) *Phosphorus: The Carbon Copy* (Eds.: K. Dillon, F. Mathey, J. F. Nixon), Wiley, Chichester, **1998**; b) *Houben Weyl, Methods of Organic Chemistry, Vols. E1 & E2: Organic Phosphorus Compounds I & II* (Ed.: M. Regitz), Thieme, Stuttgart, **1982**; c) F. Mathey, A. Sevin, *Molecular Chemistry of the Transition Metals*, Wiley, Chichester, **1996**.

[19] a) F. Mathey, *Angew. Chem.* **2003**, *115*, 1616–1643; *Angew. Chem. Int. Ed.* **2003**, *42*, 1578–1604; b) D. P. Gates, *Top. Curr. Chem.* **2005**, *250*, 107–126; c) M. Hissler, P. W. Dyer, R. Réau, *Top. Curr. Chem.* **2005**, *250*, 127–163; d) Z. Jin, B. L. Lucht, *J. Organomet. Chem.* **2002**, *653*, 167–176; e) M. G. Hobbs, T. Baumgartner, *Eur. J. Inorg. Chem.* **2007**, 3611–3628.

[20] a) C. Hay, D. Le Vilain, V. Deborde, L. Toupet, R. Réau, *Chem. Commun.* **1999**, 345–346; b) C. Hay, C. Fischmeister, M. Hissler, L. Toupet, R. Réau, *Angew. Chem.* **2000**, *112*, 1882–1885; *Angew. Chem. Int. Ed.* **2000**, *39*, 1812–1815; c) C. Hay, M. Hissler, C. Fischmeister, J. Rault-Berthelot, L. Toupet, L. Nyulászi, R. Réau, *Chem. Eur. J.* **2001**, *7*, 4222–4236; d) C. Fave, M. Hissler, T. Kárpáti, J. Rault-Berthelot, V. Deborde, L. Toupet, L. Nyulászi, R. Réau, *J. Am. Chem. Soc.* **2004**, *126*, 6058–6063; e) V. Lemau de Talance, M. Hissler, L.-Z. Zhang, T. Kárpáti, L. Nyulászi, D. Caras-Quintero, P. Bäuerle, R. Réau, *Chem. Commun.* **2008**, 2200–2202.

[21] a) C. Fave, T.-Y. Cho, M. Hissler, C.-W. Chen, T.-Y. Luh, C.-C. Wu, R. Réau, *J. Am. Chem. Soc.* **2003**, *125*, 9254–9255; b) H.-C. Su, O. Fadhel, C.-J. Yang, T.-Y. Cho, C. Fave, M. Hissler, C.-C. Wu, R. Réau, *J. Am. Chem. Soc.* **2006**, *128*, 983–995.

[22] a) T. Baumgartner, T. Neumann, B. Wirges, *Angew. Chem.* **2004**, *116*, 6323–6328; *Angew. Chem. Int. Ed.* **2004**, *43*, 6197–6201; b) T.

Baumgartner, W. Bergmans, T. Kárpáti, T. Neumann, M. Nieger, L. Nyulászi, *Chem. Eur. J.* **2005**, *11*, 4687–4699.
[23] a) T. Baumgartner, *J. Inorg. Organomet. Polym. Mater.* **2005**, *15*, 389–409; b) X. Zhang, A. J. Matzger, *J. Org. Chem.* **2003**, *68*, 9813–9815; c) S. Y. Hong, J. M. Song, *J. Chem. Phys.* **1997**, *107*, 10607–10615.
[24] a) T. Baumgartner, W. Wilk, *Org. Lett.* **2006**, *8*, 503–506; b) Y. Dienes, M. Eggenstein, T. Neumann, U. Englert, T. Baumgartner, *Dalton Trans.* **2006**, 1424–1433; c) T. Neumann, Y. Dienes, T. Baumgartner, *Org. Lett.* **2006**, *8*, 495–497; d) S. Durben, Y. Dienes, T. Baumgartner, *Org. Lett.* **2006**, *8*, 5893–5896; e) Y. Dienes, S. Durben, T. Kárpáti, T. Neumann, U. Englert, L. Nyulászi, T. Baumgartner, *Chem. Eur. J.* **2007**, *13*, 7487–7500.
[25] U. Dahlmann, R. Neidlein, *Helv. Chim. Acta* **1997**, *80*, 111–120.
[26] J. R. Lakowicz, *Principles of Fluorescence Spectroscopy*, 3rd ed., Springer, New York **2006**.
[27] A. B. Koren, M. D. Curtis, A. H. Francis, J. W. Kampf, *J. Am. Chem. Soc.* **2003**, *125*, 5040–5050.
[28] a) D. Holmes, S. Kumaraswamy, A. J. Matzger, K. P. C. Vollhardt, *Chem. Eur. J.* **1999**, *5*, 3399–3412; b) G. Horowitz, B. Bachet, A. Yassar, P. Lang, F. Demanze, J. L. Fave, F. Garnier, *Chem. Mater.* **1995**, *7*, 1337–1341; c) T. Siegrist, R. M. Fleming, R. C. Haddon, R. A. Laudise, A. J. Lovinger, H. E. Katz, P. Bridenbaugh, D. D. Davis, *J. Mater. Res.* **1995**, *10*, 2170–2173.
[29] a) T. Yamamoto, D. Komarudin, M. Arai, B. L. Lee, H. Suganuma, N. Asakawa, Y. Inoue, K. Kubota, S. Sasaki, T. Fukuda, H. Matsuda, *J. Am. Chem. Soc.* **1998**, *120*, 2047–2058; b) J. K. Politis, J. C. Nemes, M. D. Curtis, *J. Am. Chem. Soc.* **2001**, *123*, 2537–2547.
[30] M. A. Wolak, J. H. Delcamp, C. A. Landis, P. A. Lane, J. E. Anthony, Z. H. Kafafi, *Adv. Funct. Mater.* **2006**, *16*, 1943–1949.
[31] a) M. Turbiez, P. Frère, M. Allain, N. Gallego-Planas, J. Roncali, *Macromolecules* **2005**, *38*, 6806–6812; b) M. Turbiez, P. Frère, J. Roncali, *J. Org. Chem*, **2003**, *68*, 5357–5360; c) P. Leriche, M. Turbiez, V. Monroche, P. Frère, P. Blanchard, P. J. Skabara, J. Roncali, *Tetrahedron Lett.* **2003**, *44*, 649–652; d) C. Rethore, A. Madalan, M. Fourmigue, E. Canadell, E. B. Lopes, M. Almeida, R. Clerac, N. Avarvari, *New J. Chem.* **2007**, *31*, 1468–1483; e) G. Raos, A. Famulari, S. V. Meille, M. C. Gallazzi, G. Allegra, *J. Phys. Chem. A* **2004**, *108*, 691–698; f) C. Bleiholder, D. B. Werz, H. Köppel, R. Gleiter, *J. Am. Chem. Soc.* **2006**, *128*, 2666–2674; g) C. Bleiholder, R. Gleiter, D. B. Werz, H. Köppel, *Inorg.* Chem. **2007**, *46*, 2249–2260; h) R. E. Rosenfeld, R. Parthasarathy, J. Dunitz, *J. Am. Chem. Soc.* **1977**, *99*, 4860–4862; i) R. A. Poirier, Á. Kucsman, I. G. Csizmadia, *J. Am. Chem. Soc.* **1987**, *109*, 2237–2245.
[32] P. Adkine, T. Cantat, E. Deschamps, L. Ricard, N. Mézailles, P. Le Floch, M. Geoffroy, *Phys. Chem. Chem. Phys.* **2006**, *8*, 862–868.
[33] A. Modelli, B. Hajgató, J. F. Nixon, L. Nyulászi, *J. Phys. Chem. A* **2004**, *108*, 7440–7447.
[34] Y. Xie, H. F. Schaefer III, F. A. Cotton, *Chem. Commun.* **2003**, 102–103.
[35] A. J. Bard, L. R. Faulkner, *Electrochemical Methods: Fundamentals and Applications*, 2nd ed., Wiley, New York, **2001**.
[36] T. Miyajima, Y. Matano, H. Imahori, *Eur. J. Org. Chem.* **2008**, 255–259.
[37] R. W. F. Bader, *Acc. Chem. Res.* **1985**, *18*, 9–15.
[38] G. Barbarella, L. Favaretto, A. Zanelli, G. Gigli, M. Mazzeo, M. Anni, A. Bongini, *Adv. Funct. Mater.* **2005**, *15*, 664–670.
[39] R. Usón, A. Laguna, M. Laguna, *Inorg. Synth.* **1989**, *26*, 85–91.
[40] a) A. D. Becke, *J. Chem. Phys.* **1993**, *98*, 5648; b) C. Lee, W. Yang, R. G. Parr, *Phys. Rev. B* **1988**, *37*, 785–789.
[41] Gaussian 03, Revision C.02, M. J. Frisch, G. W. Trucks, H. B. Schlegel, G. E. Scuseria, M. A. Robb, J. R. Cheeseman, J. A. Montgomery, Jr., T. Vreven, K. N. Kudin, J. C. Burant, J. M. Millam, S. S. Iyengar, J. Tomasi, V. Barone, B. Mennucci, M. Cossi, G. Scalmani, N. Rega, G. A. Petersson, H. Nakatsuji, M. Hada, M. Ehara, K. Toyota, R. Fukuda, J. Hasegawa, M. Ishida, T. Nakajima, Y. Honda, O. Kitao, H. Nakai, M. Klene, X. Li, J. E. Knox, H. P. Hratchian, J. B. Cross, V. Bakken, C. Adamo, J. Jaramillo, R. Gomperts, R. E. Stratmann, O. Yazyev, A. J. Austin, R. Cammi, C. Pomelli, J. W. Ochterski, P. Y. Ayala, K. Morokuma, G. A. Voth, P. Salvador, J. J. Dannenberg, V. G. Zakrzewski, S. Dapprich, A. D. Daniels, M. C. Strain, O. Farkas, D. K. Malick, A. D. Rabuck, K. Raghavachari, J. B. Foresman, J. V. Ortiz, Q. Cui, A. G. Baboul, S. Clifford, J. Cioslowski, B. B. Stefanov, G. Liu, A. Liashenko, P. Piskorz, I. Komaromi, R. L. Martin, D. J. Fox, T. Keith, M. A. Al-Laham, C. Y. Peng, A. Nanayakkara, M. Challacombe, P. M. W. Gill, B. Johnson, W. Chen, M. W. Wong, C. Gonzalez, J. A. Pople, Gaussian, Inc., Wallingford, CT, **2004**.

Received: July 29, 2008
Published online: October 9, 2008

